ELSEVIER

Journal of Organometallic Chemistry 513 (1996) 17–26

Journal of Organometallic Chemistry

Reaction of (POR)M(OAc)$_2$ (M = Zr, Hf) with ^{n}BuLi and solid state structure of [(TPP)Zr(μ-OH)$_2$]$_2$

Jean L. Huhmann [a,*], Joyce Y. Corey [a], Nigam P. Rath [a], Charles F. Campana [b]

[a] *University of Missouri-St. Louis, St. Louis, MO 63121, USA*

[b] *Siemens Industrial Automation, 6300 Enterprise Lane, Madison, WI 53719, USA*

Received 24 March 1995; in revised form 3 July 1995

Abstract

A general route to (TPP)Zr(OAc)$_2$, (OEP)Zr(OAc)$_2$ and (TPP)Hf(OAc)$_2$ from the reaction of MCl_4 and H_2(POR) in benzonitrile, followed by treatment with pyridine + acetic acid is described. The reaction of (POR)M(OAc)$_2$ with ^{n}BuLi occurs in a stepwise manner, with approximately 2 equiv. of ^{n}BuLi required before the formation of M(^{n}Bu) is observed, and 4 equiv. required for stoichiometric conversion to (POR)M(^{n}Bu)$_2$. The tetrahydroxo-bridged dimer [(TPP)Zr(μ-OH)$_2$]$_2$ was obtained as the benzene solvate from the hydrolysis of (TPP)Zr(^{n}Bu)$_2$, and the structure was determined by single crystal X-ray diffraction (triclinic, $P\bar{1}$; a = 10.606(2) Å, b = 13.003(3) Å, c = 14.587(3) Å, α = 99.85(3)°, β = 107.61(3)°, γ = 96.82(3)°, Z = 2).

Keywords: Porphyrin; Zirconium; Hafnium; Silane

1. Introduction

The organometallic chemistry of the early transition metal porphyrins has lagged behind that of the corresponding late transition metal derivatives, largely due to their high oxophilicity and ease of hydrolysis [1]. There has been a growing interest in the development of Zr and Hf porphyrins, a useful feature of which is the availability of *cis* forms of (POR)MX_2 (POR = porphyrin dianion), such as (TPP)MCl_2 (TPP = *meso*-tetraphenyl porphyrin) and (OEP)MCl_2 (OEP = octaethylporphyrin) [2]. Furthermore, the structure and reactivity for such Zr and Hf metalloporphyrins could be related to that of the versatile Group 4 metallocenes Cp_2MCl_2 (Fig. 1(a,b)) [2a,2c,3,4].

Recent investigations into the reaction chemistry of Zr and Hf porphyrins have provided several organometallic compounds. The Zr complexes are obtained primarily from a salt elimination reaction between RM′ and (POR)$ZrCl_2$. For example, the σ-bonded complexes (OEP)ZrR_2 (R = Me, Et, CH_2SiMe3, p-C_6H4^tBu) [2c], (TPP)$ZrMe_2$ [2a], and π-bonded complexes (OEP)Zr(COT) [2c] and (OEP)Zr(η^5-1,2-$C_2B_9H_{11}$) [2a,5] were all obtained from the reaction of (POR)$ZrCl_2$ with a Li, Na, K, Mg, or Tl salt of R. Similarly, reaction of (TPP)$HfCl_2$ with MeLi provided (TPP)$HfMe_2$ [6a]. In addition, the preparation of (POR)Hf(bdt) (bdt = benzenedithiolate, POR = TPP) from the reaction of (POR)$HfCl_2$ with H_2(bdt) in the presence of Et_3N illustrates the further synthetic utility of the halide precursors [6b]. A related process has recently been described by Arnold, where Li_2(POR)(solv)$_n$ was reacted with $(Me_3SiCH_2)_2MCl_2$-(solv)$_n$ to produce (POR)M(CH_2SiMe_3)$_2$ (M = Zr, Hf; POR = TPP, OEP; solv = Et_2O, THF) [7]. The dichloro-substituted Zr and Hf metalloporphyrins employed as starting materials in the majority of these reactions were prepared from the reaction of [Li(THF)$_4$][Li(POR)] with [MCl_4(solv)$_2$] (solv = THF, THT) [2]. One disadvantage of using (POR)MCl_2 as a starting point for the synthesis of organometallic complexes is that the Zr and Hf porphyrin dichlorides are

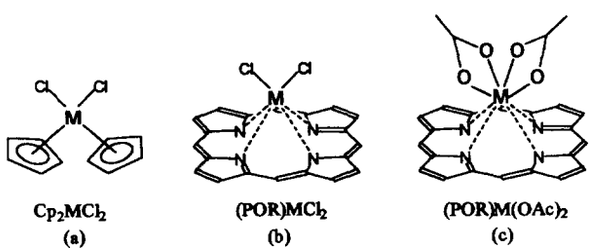

Fig. 1.

* Corresponding author.

SSDI 0022-328X(95)05835-4

easily hydrolyzed, leading to difficulties in purification and storage.

We sought an alternative entry to organometallic Zr and Hf porphyrin complexes through the diacetate derivatives, (POR)M(OAc)$_2$, which are air and moisture stable, and may be easily stored and handled. The Zr and Hf porphyrin diacetates have been shown to possess two bidentate $^-O_2CCH_3$ ligands, and because these ligands are oriented in a *cis* configuration, (POR)M(OAc)$_2$ may also be considered related to Cp_2MCl_2 (Fig. 1(c)) [8]. Along these lines, an earlier study by Inoue presented NMR evidence that the reaction of (TPP)Zr(OAc)$_2$ with a large excess (9 equiv.) of RLi produced (TPP)ZrR$_2$ (R = Me, ^{n}Bu, Et, Ph) [9]. However, little of the reaction chemistry of Zr and Hf porphyrin diacetates has been developed, and a general method leading to the isolation of organometallic compounds from reactions with (POR)M(OAc)$_2$ has not yet been established. In this study, we report a general synthesis of (POR)M(OAc)$_2$ (M = Zr; POR = TPP, OEP; M = Hf; POR = TPP) and reactions of these porphyrin diacetates with ^{n}BuLi, CH_3COOH and HCl.

2. Results

2.1. Synthesis of (POR)M(OAc)$_2$

The porphyrin diacetates (TPP)Zr(OAc)$_2$, (OEP)Zr(OAc)$_2$ and (TPP)Hf(OAc)$_2$ were prepared in high yields (82–92%) from MCl_4 and H_2(POR) in refluxing benzonitrile, followed by reaction of the concentrated benzonitrile solution with a boiling acetic acid + pyridine mixture. The crude product crystallized from the reaction mixture after the addition of boiling water to provide bright pink or purple plates. The general reaction sequence is summarized in Eq. (1).

$$H_2(POR) + MCl_4 \xrightarrow[2)\ \text{acetic acid/pyridine},\Delta \\ 3)\ H_2O,\Delta]{1)\ \text{Benzonitrile},\Delta} \begin{matrix}(POR)M(OAc)_2 \\ (TPP)Zr,\ 82\% \\ (TPP)Hf,\ 92\% \\ (OEP)Zr,\ 88\%\end{matrix} \quad (1)$$

An excess of MCl_4 was used to drive the consumption of H_2(POR), as it is difficult to cleanly separate the product (POR)M(OAc)$_2$ from the starting porphyrin. The initial mixing of H_2(TPP) with MCl_4 in benzonitrile produced a bright green solution for both Zr and Hf, which indicated the formation of $H_4(TPP)^{2+}$ (identified by the characteristic UV-vis spectra) [10]. The green color gradually darkened upon reflux and eventually turned dark red, presumably forming the dichloride (TPP)MCl_2 [11], which was not isolated from the benzonitrile solution but concentrated and dissolved in acetic acid + pyridine. In contrast, the mixture of H_2(OEP) with $ZrCl_4$ immediately turned dark red upon mixing in benzonitrile, and the intermediate formation of $H_4(OEP)^{2+}$ was not observed.

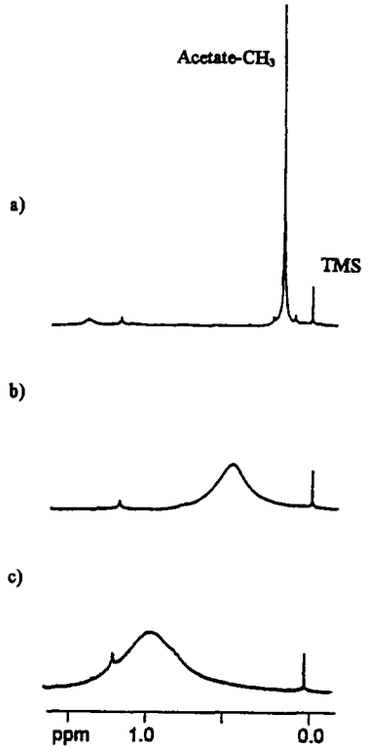

Fig. 2. ^{1}H-NMR (300 MHz, $CDCl_3$) spectra, acetate region only. (a) (TPP)Zr(OAc)$_2$; (b) after addition of 0.4 equiv. of HOAc to (a); (c) after addition of 1.2 equiv. of HOAc to (a).

The ^{1}H-NMR, ^{13}C-NMR and UV-vis spectroscopic data for (TPP)Zr(OAc)$_2$ and (OEP)Zr(OAc)$_2$ prepared according to Eq. (1) match those described in the literature [2c,4,12]. The Hf derivative, (TPP)Hf(OAc)$_2$, which was previously unreported, provided satisfactory elemental analysis and exhibited spectroscopic data that were very similar to those obtained for (TPP)Zr(OAc)$_2$.

2.2. Acetic acid exchange with (POR)M(OAc)$_2$

Suprisingly, the initial crystals obtained from the dropwise addition of boiling water to the (POR)M(OAc)$_2$ acetic acid + pyridine solutions did not exhibit the expected ^{1}H-NMR resonance for the acetate–CH_3 groups. This was found to result from an exchange between coordinated acetate and residual acetic acid. The residual acid was removed from the Hf complex by heating under vacuum, but the Zr complexes required elution of $CHCl_3$ solutions through a short SiO_2 plug. Once the residual acid was removed, a sharp resonance associated with the methyl group of the coordinated acetate was observed. As an example of this exchange, Fig. 2 demonstrates the effect that sequential addition of HOAc has on the ^{1}H-NMR resonance of the coordinated acetate for (TPP)Zr(OAc)$_2$ in $CDCl_3$ solution. All three diacetate derivatives described in this paper exhibited this exchange.

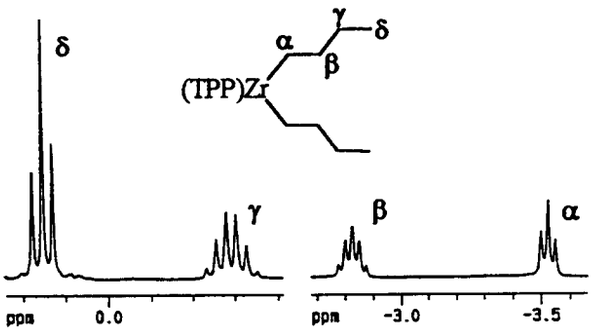

Fig. 3. Partial ^{1}H-NMR (300 MHz, C_7D_8) spectrum of (TPP)Zr(^{n}Bu)$_2$ formed from the addition of 2 equiv. of ^{n}BuLi to (TPP)ZrCl$_2$.

of hexanes provided almost quantitative conversion to (TPP)ZrCl$_2$ (95% yield). The reaction proceeded with a color change from bright red to burgundy, and the final dichloride product was obtained as a red powder. The NMR and UV-vis spectral data matched those reported in the literature for (TPP)ZrCl$_2$, prepared from [Li(THF)$_4$][Li(TPP)] and [ZrCl$_4$(THF)$_2$] [2a]. Reaction of (TPP)Hf(OAc)$_2$ with HCl under similar conditions produced a dark purple solid, which proved to be a mixture of (TPP)Hf(OAc)$_2$ and (TPP)HfCl$_2$ in approximately a 1:2 ratio, as determined by ^{1}H-NMR. The ^{1}H-NMR peaks assigned to the dichloride matched those reported in the literature for (TPP)HfCl$_2$, prepared from [Li(THF)$_4$][Li(TPP)] with [HfCl$_4$(THF)$_2$] [2b]. Under the same conditions, reaction of (OEP)Zr(OAc)$_2$ with HCl produced no identifiable products.

2.4. Reactions of (POR)ZrCl$_2$ and (POR)M(OAc)$_2$ with ^{n}BuLi

When 2 equiv. of ^{n}BuLi were added to (TPP)ZrCl$_2$ in C_7D_8, resonances attributed to σ-bonded ^{n}Bu groups for (TPP)Zr(^{n}Bu)$_2$ appeared as well resolved first order multiplets between 0.2 and −4.0 ppm (Fig. 3). The integrated ratio of the sum of the α- and β-^{n}Bu protons to the β-pyrrole protons of the porphyrin was 1:1, confirming the presence of 2 coordinated ^{n}Bu groups per (TPP)Zr unit.

When 2 equiv. of ^{n}BuLi were added to (TPP)Zr(OAc)$_2$, (OEP)Zr(OAc)$_2$ or (TPP)Hf(OAc)$_2$, intermediate products were obtained, as indicated by multiple resonances in the porphyrin regions of the ^{1}H-NMR spectra and ratios of coordinated ^{n}Bu to (POR)M of less than 1:1. However, when 4 equiv. of

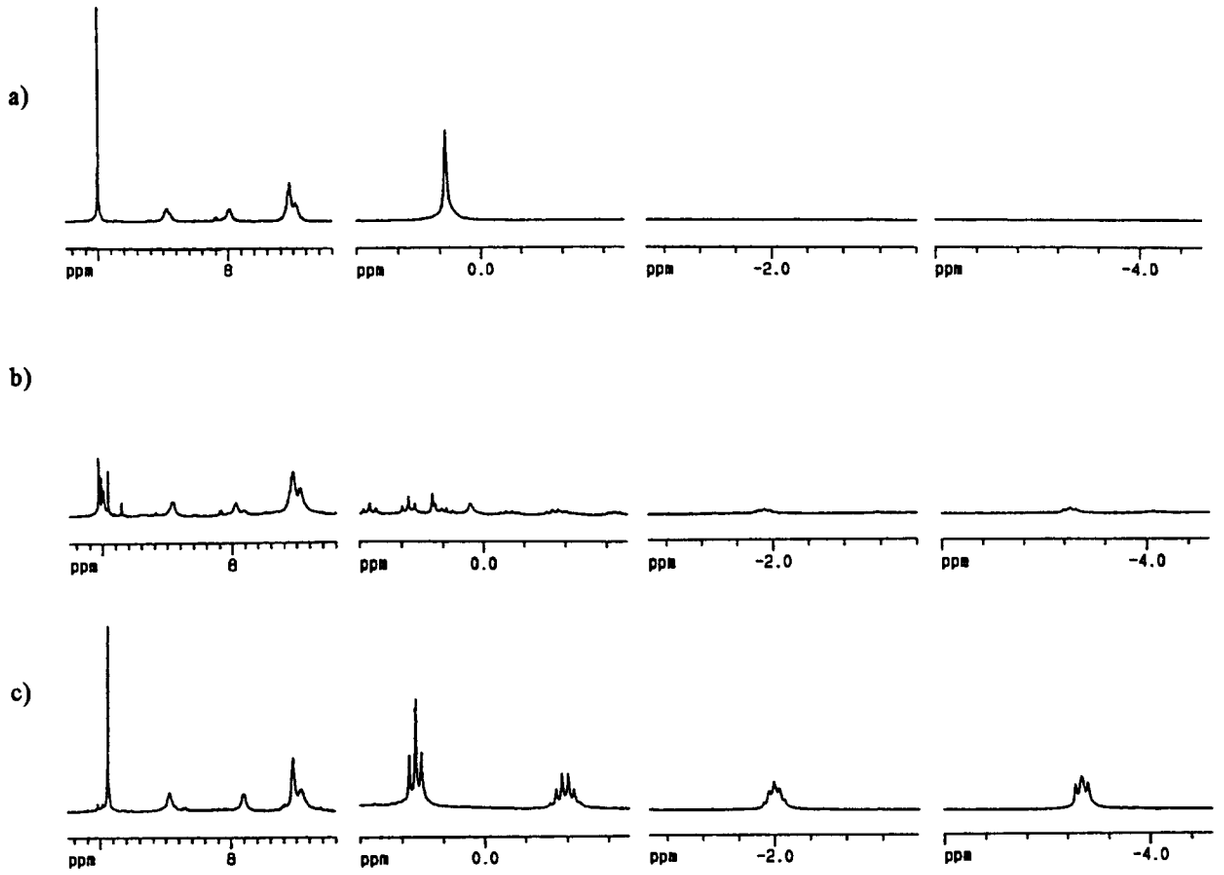

Fig. 4. Partial ^{1}H-NMR (500 MHz, C_7D_8) spectra of stepwise reaction of (TPP)Hf(OAc)$_2$ with ^{n}BuLi. (a) (TPP)Hf(OAc)$_2$; (b) after addition of 2 equiv. of ^{n}BuLi to (a); (c) after addition of 4 equiv. of ^{n}BuLi to (a).

^{n}BuLi had been added to (POR)M(OAc)$_2$, the ratio of coordinated ^{n}Bu to (POR)M became 2:1, signifying the formation of the σ-bonded dibutyl complexes (POR)M(^{n}Bu)$_2$. The ^{1}H-NMR spectra shown in Fig. 4 illustrate this stepwise reaction of ^{n}BuLi with (POR)M(OAc)$_2$ for (TPP)Hf(OAc)$_2$, and similar data were obtained from reaction with (TPP)Zr(OAc)$_2$ and (OEP)Zr(OAc)$_2$. Finally, the porphyrin and butyl regions in the ^{1}H-NMR for the product obtained from the addition of 4 equiv. of ^{n}BuLi to (TPP)Zr(OAc)$_2$ are identical to those obtained from the addition of 2 equiv. of ^{n}BuLi to (TPP)ZrCl$_2$, confirming the formation of (TPP)Zr(^{n}Bu)$_2$ from the diacetate.

2.5. Hydrolysis of (TPP)Zr(^{n}Bu)$_2$ and solid state structure of [(TPP)Zr(μ-OH)$_2$]$_2$[C$_6$H$_6$]

When a solution of (TPP)Zr(^{n}Bu)$_2$ was kept at 5°C in benzene solution for 1 month, small purple crystals deposited. The crystals were sparingly soluble in $CHCl_3$, CH_2Cl_2 and C_7H_8, and insoluble in THF and hexanes. The ^{1}H-NMR spectrum of the crystals in $CDCl_3$ showed an upfield shift of the pyrrole protons to 8.42 ppm, and a signal at −6.79 ppm which was assigned to bridging OH groups. The FT-IR spectrum in KBr exhibited a weak O–H band at 3577 cm^{-1}. These data are consistent with those observed for hydroxo-bridged porphyrin dimers, such as described by Kim for [(TPP)Zr]$_2$(μ-OH)$_2$(μ-O) [13].

A single crystal X-ray diffraction study showed the crystals to be a benzene solvate of the tetra-hydroxo bridged dimer [(TPP)Zr(μ-OH)$_2$]$_2$, which was presumed to form upon hydrolysis of the metal alkyl. Experimental details of the structure determination are provided in Table 1, and the atomic coordinates for non-hydrogen atoms are in Table 2. Table 3 lists selected bond lengths and angles. Two orientations of the dimer are presented as ORTEP drawings in Fig. 5.

3. Discussion

3.1. Formation and reactivity of (POR)M(OAc)$_2$

The preparation of the Zr diacetate complexes (TPP)Zr(OAc)$_2$ [4] and (OEP)Zr(OAc)$_2$ [12] has been previously described. Generally, H_2(POR) is reacted with an excess of M(acac)$_4$ (acac = acetylacetonate$^-$) in refluxing phenol to produce (POR)M(X)$_2$ (X = OPh$^-$ or acac$^-$). After treatment with aqueous NaOH and elution over Al_2O_3, the resulting residue is treated with a refluxing acetic acid + pyridine mixture to produce the diacetate derivatives, which are precipitated by the addition of boiling water. This process is outlined in Eq. (2), and is similar to that used for the preparation of

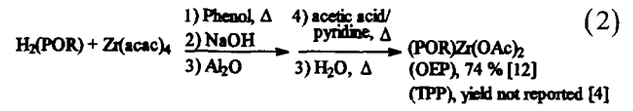

(2)

(OEP)Hf(OAc)$_2$ from H_2(OEP) and Hf(acac)$_4$ (% yield not reported) [14].

The route developed in this paper and outlined in Eq. (1) has several advantages over the literature route described in Eq. (2). First, commercially available MCl_4 is used instead of M(acac)$_4$. Second, this method does not require the isolation of the intermediate product from the reaction of MCl_4 with H_2(POR), eliminating the problems associated with removing high boiling, coordinating solvents. Lastly, the overall yields are slightly higher (82–92% vs. 74%).

The conversion of (TPP)Zr(OAc)$_2$ to (TPP)ZrCl_2 with HCl gas in $CHCl_3$ has been reported in the literature, and the spectroscopic data were provided, although no experimental details were provided [4]. In this paper, we describe the nearly quantitative conversion of (TPP)Zr(OAc)$_2$ to (TPP)ZrCl_2 (95% yield) by reaction with HCl in CH_2Cl_2 solution, followed by precipitation with an HCl saturated hexane solution. In contrast to the Zr case, the reaction of (TPP)Hf(OAc)$_2$ with HCl did not result in complete conversion to the dichloride. Instead, a mixture of (TPP)Hf(OAc)$_2$ and (TPP)HfCl_2 was obtained. This difference in reactivity toward HCl for the Zr and Hf porphyrin diacetates is most probably due to the differences in M–Cl bond strengths. The Hf–Cl bond in (TPP)HfCl_2 is weaker than the Zr–Cl bond in (TPP)ZrCl_2 [11b]. Therefore, (TPP)Zr(OAc)$_2$ is converted almost quantitatively to (TPP)ZrCl_2, whereas (TPP)Hf(OAc)$_2$ remains in equilibrium with (TPP)HfCl_2.

Table 1
Crystallographic data for [(TPP)Zr(μ-OH)$_2$]$_2$[C$_6$H$_6$]

Crystal system	Triclinic
Space group	$P\bar{1}$
a (Å)	10.606(2)
b (Å)	13.003(3)
c (Å)	14.587(3)
α (°)	99.85(3)
β (°)	107.61(3)
γ (°)	96.82(3)
V (Å^3)	1857.8(7)
Z	2
D_c (g cm^{-3})	1.389
T (K)	293(2)
Radiation	Mo Kα (λ = 0.71073 Å)
μ (mm^{-1})	0.342
2θ range (ε)	3.0 to 45.0
Reflections collected	6080
Independent reflections	4689 (R_{int} = 0.0416)
Data/restraints/parameters	4518/0/488
Final R indices [I > 2σ I]	$R(F)$ = 0.0920
R indices (all data)	$wR(F^2)$ = 0.3165
Goodness of fit (F^2)	1.04

Curiously, the analogous reaction of $(OEP)Zr(OAc)_2$ with HCl did not produce $(OEP)ZrCl_2$. Instead, dark colored insoluble decomposition products were obtained. However, Arnold has recently described the conversion of $(OEP)Zr(OAc)_2$ to $(OEP)ZrCl_2$ with $SiCl_4$, as well as the conversion of $(OEP)ZrCl_2(0.5Tol)$ back to the diacetate $(OEP)Zr(OAc)_2$ with NaOAc in HOAc [2c].

Table 2
Atomic coordinates ($\times 10^4$) and equivalent isotropic displacement parameters ($Å^2 \times 10^3$) for $[(TPP)Zr(\mu\text{-}OH)_2]_2$

	x	y	z	U_{eq} [a]
Zr	3945(1)	9782(1)	495(1)	30(1)
O(1)	5324(18)	11133(10)	511(13)	135(6)
O(2)	5986(13)	9819(18)	813(9)	167(9)
N(1)	3823(8)	8244(8)	1043(6)	32(2)
N(2)	4591(8)	10405(7)	2163(6)	31(2)
N(3)	2650(9)	11045(8)	591(6)	34(2)
N(4)	1867(8)	8915(7)	−475(6)	33(2)
C(1)	3201(11)	7275(9)	480(8)	33(3)
C(2)	3691(14)	6461(10)	995(9)	49(3)
C(3)	4593(12)	6941(10)	1850(9)	45(3)
C(4)	4706(11)	8808(10)	1906(8)	36(3)
C(5)	5426(11)	8851(10)	2731(8)	37(3)
C(6)	5362(11)	9953(11)	2845(7)	41(3)
C(7)	6052(13)	10714(10)	3710(9)	47(3)
C(8)	5662(13)	11665(11)	3592(9)	50(3)
C(9)	4731(11)	11455(9)	2586(7)	30(3)
C(10)	4091(11)	12221(10)	2173(8)	36(3)
C(11)	3154(11)	11996(9)	1224(8)	34(3)
C(12)	2507(14)	12805(10)	789(8)	49(3)
C(13)	1644(12)	12310(10)	−105(8)	42(3)
C(14)	1707(11)	11184(10)	−234(8)	36(3)
C(15)	926(11)	10403(10)	−1026(8)	37(3)
C(16)	984(11)	9320(10)	−1116(8)	37(3)
C(17)	18(13)	8527(11)	−1872(9)	52(4)
C(18)	349(13)	7556(11)	−1722(9)	50(3)
C(19)	1528(11)	7824(10)	−827(8)	37(3)
C(20)	2122(12)	7043(9)	−415(8)	36(3)
C(21)	6331(11)	8527(10)	3606(7)	34(3)
C(22)	7403(12)	8070(10)	3512(9)	47(3)
C(23)	8217(15)	7740(13)	4301(10)	65(4)
C(24)	7949(14)	7814(12)	5148(10)	62(4)
C(25)	6883(15)	8238(12)	5232(9)	60(4)
C(26)	6099(12)	8584(11)	4459(8)	48(3)
C(27)	4442(12)	13325(9)	2748(7)	35(3)
C(28)	5700(15)	13936(12)	3007(10)	58(4)
C(29)	6002(19)	14930(13)	3552(12)	74(5)
C(30)	5091(23)	15387(12)	3864(10)	77(6)
C(31)	3829(20)	14810(14)	3642(11)	79(5)
C(32)	3518(14)	13793(10)	3089(9)	50(3)
C(33)	−47(10)	10713	−1893(7)	32(3)
C(34)	−1075(11)	11198(11)	−1805(8)	46(3)
C(35)	−1934(13)	11507(13)	−2601(10)	60(4)
C(36)	−1745(13)	11301(12)	−3485(9)	55(4)
C(37)	−718(14)	10797(12)	−3593(8)	57(4)
C(38)	130(13)	10511(10)	−2812(9)	47(3)
C(39)	1654(12)	5915(9)	−951(8)	37(3)
C(40)	400(13)	5396(10)	−1077(9)	48(3)
C(41)	−24(15)	4375(12)	−1554(10)	60(4)
C(42)	771(18)	3817(12)	−1951(10)	66(4)
C(43)	2010(18)	4303(12)	−1828(10)	65(4)
C(44)	2460(14)	5354(11)	−1340(10)	53(4)
C(45)	9(53)	4742(69)	4160(27)	179(20)
C(46)	824(55)	5870(60)	4664(36)	234(37)
C(47)	−750(55)	3864(51)	4475(76)	277(34)

[a] U_{eq} is defined as one-third of the trace of the orthogonalized U_{ij} tensor.

Table 3
Selected bond lengths and bond angles for $[(TPP)Zr(\mu\text{-}OH)_2]_2$

Bond lengths (Å)		Bond angles (°)	
Zr–O(1)	2.14(2)	O(1)–Zr–O(2)	56.5(7)
Zr–O(2)	2.064(13)	O(2)–Zr–O(1A)	59.8(7)
Zr–O(1A)	2.116(13)	O(1)–Zr–O(2A)	59.1(6)
Zr–O(2A)	2.081(13)	O(1)–Zr–O(1A)	88.2(5)
Zr–N(1)	2.281(10)	O(2)–Zr–O(2A)	85.0(6)
Zr–N(2)	2.288(8)	N(1)–Zr–N(2)	78.3(3)
Zr–N(3)	2.275(9)	N(2)–Zr–N(3)	78.8(3)
Zr–N(4)	2.259(9)	N(3)–Zr–N(4)	77.0(3)
Zr–ZrA	3.057(2)	N(1)–Zr–N(4)	78.6(3)
		Zr–O(1)–ZrA	91.8(5)
		Zr–O(2)–ZrA	95.0(6)

3.2. Formation of $(POR)M(^nBu)_2$

The general reaction of $(POR)MCl_2$ with RLi has been described in the literature and used as a route for the preparation of organometallic Zr and Hf complexes $(POR)MR_2$ (M = Zr, R = Me, CH_2SiMe_3, and *p*-$C_6H_4^tBu$; M = Hf, R = Me), and in all of these cases 2 equiv. of RLi were required for complete conversion to the dialkyl complex [2,6]. This was also observed for the conversion of $(TPP)ZrCl_2$ to $(TPP)Zr(^nBu)_2$ with 2 equiv. of ^{n}BuLi, as described in the current study. The dibutyl complex $(TPP)Zr(^nBu)_2$ was not isolated from the reaction mixture, but was identified by the characteristic proton ^{n}Bu multiplets (see Fig. 3), which were observed in the ^{1}H-NMR spectrum between 0.2 and −4.0 ppm. The upfield shift of the ^{n}Bu resonances has been attributed to the strong shielding effect of the porphyrin ligand [2c].

In NMR studies, the conversion of $(TPP)Zr(OAc)_2$ to $(TPP)ZrR_2$ with a large excess (9 equiv.) of RLi (R = Me, Et, Ph, ^{n}Bu) was described in a brief report by Inoue [9]. We found that the reaction is complete with the addition of 4 equiv. of ^{n}BuLi, and at least 2 equiv. are required for any appreciable concentration of $(TPP)Zr(^nBu)_2$ to be observed. In fact, after the addition of 2 equiv. of ^{n}BuLi, the ratio of Zr coordinated ^{n}Bu to (TPP)Zr unit was only 0.1:1, but after the addition of 4 equiv, the ratio was 2:1. These results suggest that the first 2 equiv. of ^{n}BuLi react with the coordinated acetate ligands, and the second 2 equiv. of ^{n}BuLi react with the Zr. Similar reactivity was observed for the addition of 2 and 4 equiv. of ^{n}BuLi to $(TPP)Hf(OAc)_2$ and $(OEP)Zr(OAc)_2$, except that the ratio of coordinated ^{n}Bu to (POR)M unit after the addition of the first 2 equiv. was 0.3:1 for (TPP)Hf and 0.8 for (OEP)Zr, and 2:1 for both after the addition of 4 equiv. ^{n}BuLi.

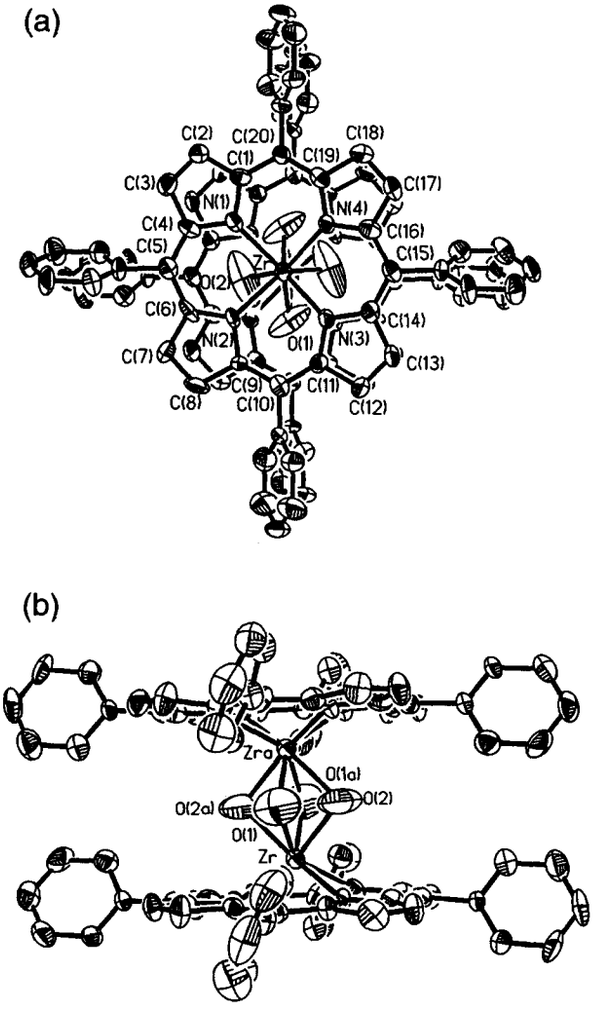

Fig. 5. Projections of $[(TPP)Zr(\mu\text{-}OH)_2]_2$. (a) top view; (b) side view. Thermal ellipsoids are drawn to 50% probability.

3.3. Reactions of $(TPP)Zr(^nBu)_2$ with $PhMe_2SiH$ and H_2O

It has been demonstrated that dialkyl zirconocenes such as $Cp_2Zr(^nBu)_2$ decompose near room temperature via β-hydride elimination to produce the olefin complex Cp_2Zr(butene), which may be intercepted with $PhMe_2SiH$ to provide the hydrosilylzirconium dimer $[Cp_2Zr(H)(SiPhMe_2)]_2$ [15]. Furthermore, Cp_2Zr(butene) acts as a catalyst for the conversion of R_2SiH_2 (R = H, Ph, Me, Et) to silicon oligomers through dehydrocoupling [16]. Our study was originally motivated by the expectation that $(POR)Zr(^nBu)_2$ would react in an analogous manner, and that the development of $(POR)Zr(^nBu)_2$ as a catalyst precursor for the dehydrocoupling of hydrosilanes to silicon oligomers would be possible. However, $(TPP)Zr(^nBu)_2$ seems to be considerably more thermally stable than $Cp_2Zr(^nBu)_2$, and also shows no reaction with $PhMe_2SiH$. In fact, decomposition of the dialkyl porphyrin complex is not observed below 80°C. It is possible that the decomposition of $(TPP)Zr(^nBu)_2$ proceeds by a route other than β-hydride elimination, accounting for the lack of reactivity toward $PhMe_2SiH$.

Although $(TPP)Zr(^nBu)_2$ appears to be quite thermally stable in aromatic solvents, it proved to be susceptible to hydrolysis, and attempts to obtain crystals of the dibutyl complex were unsuccessful. One such attempt resulted in the isolation of a small amount of dark purple cubic shaped crystals of medium quality which were satisfactory for a single crystal X-ray diffraction study. The structure was determined to be a benzene solvate of the first tetrahydroxo bridged porphyrin dimer, $[(TPP)Zr(\mu\text{-}OH)_2]_2[C_6H_6]$ as illustrated in Fig. 5. Fig. 5a shows the approximate square-antiprismatic environment about the Zr center, with the four bridging oxygens forming one square of the face, and the four nitrogens of the porphyrin ring forming the other square face. The porphyrins are eclipsed and the bridging oxygens are disordered, as are the carbons in the benzene solvent molecule [17].

The structure of this dimer is similar to that reported for the oxygen bridged dimers $[(TPP)M]_2(\mu\text{-}OH)_2(\mu\text{-}O)$ (M = Zr [13], Hf [6a]) and $[(OEP)Zr]_2(\mu\text{-}OH)_3(7,8\text{-}C_2B_9H_{12})$ [13], which were isolated from attempts to crystallize $(TPP)MMe_2$ and $(OEP)Zr(\eta^5\text{-}C_2B_9H_{11})$ re-

Table 4
Comparison of parameters in oxygen-bridged Zr and Hf porphyrin dimers

Parameter	$[(TPP)Zr(\mu\text{-}OH)_2]_2$ [a]	$[(TPP)Hf]_2(\mu\text{-}OH)_2(\mu\text{-}O)$ [b]	$[(TPP)Zr]_2(\mu\text{-}OH)_2(\mu\text{-}O)$ [c]	$[(OEP)Zr]_2(\mu\text{-}OH)_3^+$ [d]
M–O (oxo) (Å)	–	1.98	1.98	–
M–O (hydroxo) (Å)	2.14 (av)	2.19 (av)	2.18 (av)	2.15 (av)
M–O–M′ (oxo) (°)	–	101.6	101.7	–
M–O–M′ (hydroxo) (°)	91.4 (av)	88.9	89.7	98.2 (av)
M–M′ (Å)	3.06	3.06	3.07	3.25
M–N_4 plane (Å)	1.03	1.05	1.06	0.94
M–N (Å)	2.28 (av)	2.27 (av)	2.29 (av)	2.22 (av)
N–M–M′–N′ (torsion) (°)	0.6 [e]	9.5	7.8	0.7

[a] This work. [b] Ref. [6a]. [c] Ref. [13]. [d] Counterion is $7,8\text{-}C_2B_9H_{12}^-$, Ref. [13]. [e] N(1)–Zr–Zr′–N(3)′.

spectively. A comparison of selected parameters for these three dimers and the new tetrahydroxo-bridged dimer is given in Table 4. All four structures have essentially eclipsed porphyrin rings, with the $[(TPP)M]_2(\mu\text{-}OH)_2(\mu\text{-}O)$ exhibiting a slight twist about the M–M axis, and the shortest Zr–Zr distance is observed in the tetra-hydroxo bridged complex.

In a different study, the Zr compound $(OEP)Zr(CH_2\text{-}SiMe_3)_2$ produced a mixture of products upon hydrolysis, and the bridged dimers $[(OEP)Zr]_2(\mu\text{-}OH)_2(\mu\text{-}O)$ and $[(OEP)Zr(\mu\text{-}O)]_2$ were identified by NMR, but not characterized crystallographically [2c]. Hydrolysis can be quite complicated, and a number of products could be formed. Scheme 1 shows several possible reaction pathways for the hydrolysis of $(POR)MR_2$ ($R = {}^n$Bu) leading to di-, tri-, and tetra-bridging dimers.

Other related oxygen bridged pophyrin dimers have been reported in the literature. For example, $[(OEP)Sc(\mu\text{-}OH)]_2$, which was obtained from the hydrolysis of $(OEP)ScN(SiMe_3)_2$ and characterized by X-ray crystallography, also exhibits eclipsed porphyrin rings [18]. Data for a series of later transition metal mono-oxygen bridged porphyrin dimers have recently been described [19].

4. Summary

The air and moisture stable $(POR)M(OAc)_2$ diacetates offer a convenient entry into organometallic Zr and Hf porphyrin compounds. In this study, an improved general route to $(POR)M(OAc)_2$ from commercially available MCl_4 and $H_2(POR)$ has been developed for $(TPP)Zr(OAc)_2$, $(OEP)Zr(OAc)_2$ and $(TPP)Hf(OAc)_2$. It was demonstrated for these three compounds that reaction with ^{n}BuLi occurs in a stepwise manner, with approximately 2 equiv. of ^{n}BuLi required before the formation of metal coordinated ^{n}Bu is detected in measurable concentrations, and 4 equiv. required for complete conversion to $(POR)M(^nBu)_2$. The dibutyl complexes are quite thermally stable, but undergo hydrolysis, and for the case of $(TPP)Zr(^nBu)_2$, the tetrahydroxo-bridged dimer $[(TPP)Zr(\mu\text{-}OH)_2]_2$ was obtained as the benzene solvate and characterized by X-ray crystallography.

5. Experimental

General considerations.

All reactions unless otherwise noted were carried out under an atmosphere of N_2 using standard Schlenk techniques. Solvents were dried using standard methods, and all glassware was flame dried before use. Commercial compounds $ZrCl_4$, $HfCl_4$, C_6H_5CN (anhydrous), CH_3COOH, and C_5H_5N were used as supplied; ^{n}BuLi was purchased in hexanes and the concentration determined by titration before use; $PhMe_2SiH$ was prepared according to a literature procedure [20]; H_2TPP was prepared according to a literature procedure [21] and purified by elution over silica gel with hexanes–$CHCl_3$ (1:5). A sample of H_2OEP was graciously supplied by R. Guillard.

^{1}H- and ^{13}C-NMR data were recorded in $CDCl_3$ (referenced to $CHCl_3$) or C_7D_8 (referenced to C_7D_7H quintet) on either an XL-300 Varian spectrometer equipped with a four nucleus probe, or a Bruker ARX500 equipped with either an inverse probe or a broad band probe. UV-vis data were collected on a Hitachi U-3100 spectrophotometer in $CHCl_3$ and are reported as λ_{max} in nm (log ε). IR data were collected

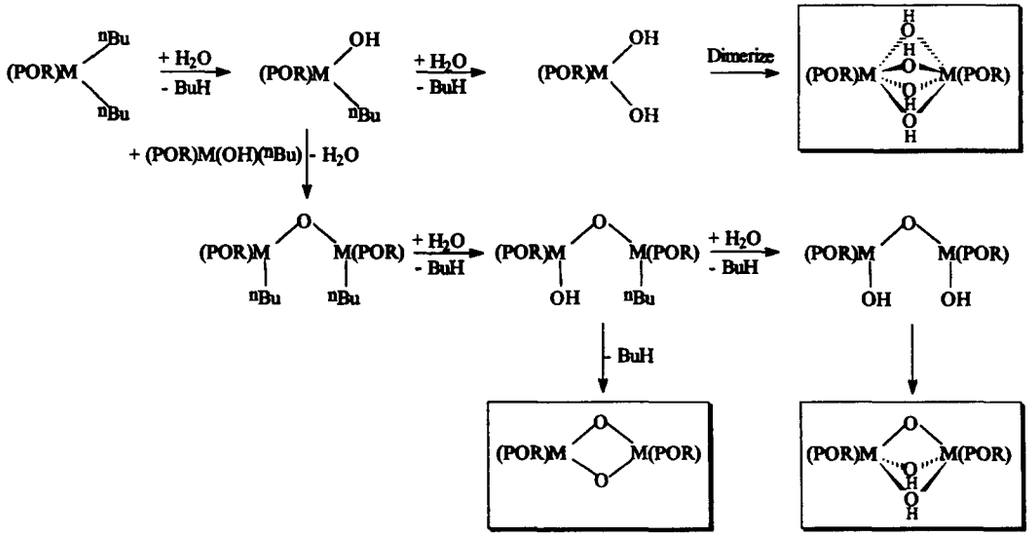

Scheme 1. Possible pathway for hydrolysis of $(POR)M(^nBu)_2$ to di-, tri- and tetra-oxygen bridged porphyrin dimers.

on a Mattson 6020 Galaxy Series FT-IR spectrometer (KBr). Elemental analysis was performed by Schwarzkopf Microanalytical Laboratories.

5.1. Synthesis of (POR)M(OAc)$_2$

Benzonitrile (10 ml) was added to a Schlenk tube containing H_2TPP (1.00 g, 1.63 mmol) and $HfCl_4$ (1.04 g, 3.25 mmol) to produce a bright green mixture which contained H_4TPP^{2+} (characteristic UV-vis bands at λ_{max} 670 nm, Soret band 443 nm). This solution was refluxed with stirring for 10 h, after which time the reaction mixture had developed an intense red color. Approximately 50% of the benzonitrile was removed by distillation under reduced pressure, and the concentrated reaction mixture was added to an Erlenmeyer flask containing pyridine (25 ml) and CH_3COOH (15 ml). The resulting dark red solution was refluxed 20 min before the dropwise addition of boiling water to provide bright pink plates, which were collected by filtration and washed with hot water and hexanes. Residual acetic acid was removed by heating under vacuum (100°C, 0.05 mmHg) for 24 h to provide pure (TPP)Hf(OAc)$_2$ (1.38 g, 92% yield). UV-vis ($CHCl_3$): 415 (5.71), 542 (4.23). ^{1}H-NMR (500 MHz, $CDCl_3$): δ 0.20 (s, 6H, acetate CH_3), 7.7–7.9 (m, 12H, *m*, *p*-phenyl), 8.10 (br d, 4H *o*-phenyl), 8.35 (br d, 4H *o*-phenyl), 8.98 (s, 8H, pyrrole). ^{13}C-NMR (125 MHz, $CDCl_3$): δ 20.9, 125.0, 126.7, 127.9, 131.3, 134.8, 142.1, 150.2 (the C=O was not observed). Anal. Calcd. for $C_{48}H_{34}O_4N_4Hf$: C, 63.40; H, 3.77; Found: C, 64.24; H, 4.02.

Analogous to the procedure above, (TPP)Zr(OAc)$_2$ (82% yield) and (OEP)Zr(OAc)$_2$ (88% yield) were obtained from the reaction of H_2(POR) with $ZrCl_4$ in refluxing benzonitrile followed by treatment with pyridine + acetic acid. The residual acetic acid was removed from the zirconium diacetates by heating under vacuum followed by filtration of $CHCl_3$ solutions through a short SiO_2 plug. The ^{1}H, ^{13}C-NMR and UV-vis spectra were identical to those reported in the literature [2c,4,12].

5.2. Reaction of (POR)M(OAc)$_2$ with acetic acid

In a septa capped NMR tube, (TPP)Zr(OAc)$_2$ (14 mg, 0.0172 mmol) was dissolved in $CDCl_3$. Acetic acid was injected in increments of 0.0070 mmol via a 10 μl syringe. The ^{1}H-NMR spectra were recorded after each addition and the results are illustrated in Fig. 3. Similar observations were obtained on addition of acetic acid to (OEP)Zr(OAc)$_2$ and (TPP)Hf(OAc)$_2$.

5.3. Reaction of (POR)M(OAc)$_2$ with HCl

Anhydrous HCl was passed through a flask containing hexanes, then through a flask containing a solution of (TPP)Zr(OAc)$_2$ (0.50 g, 0.610 mmol) in CH_2Cl_2 (200 ml) for a period of 30 min, during which time the reaction mixture turned from bright red to burgundy. The CH_2Cl_2 solution was concentrated to approximately 50 ml and the HCl saturated hexanes was added to precipitate a dark red powder. The solid was collected by filtration, washed with hexanes, and dried under vacuo (0.05 mm Hg) at 50°C overnight to provide pure (TPP)ZrCl_2 (0.45 g, 95% yield). The ^{1}H, ^{13}C-NMR and UV-vis spectra for (TPP)ZrCl_2 were identical to those reported in the literature [2a].

Analogous reaction of (TPP)Hf(OAc)$_2$ with HCl provided a mixture of (TPP)HfCl_2 and (TPP)Hf(OAc)$_2$ in a ratio of approx. 2/1 as determined by integration of the pyrrole resonances in the ^{1}H-NMR. The ^{1}H-NMR and UV-vis spectra for the (TPP)HfCl_2 were identical to those reported in the literature [2b]. Analogous reaction of (OEP)Zr(OAc)$_2$ provided no identifiable products.

5.4. Reaction of (TPP)ZrCl_2 with ^{n}BuLi

(TPP)ZrCl_2 (8.60 mg, 0.0110 mmol) was partially dissolved in C_7D_8 (1.0 ml) and a solution of ^{n}BuLi (12.0 μl, 2.0 M) was added via a 50 μl syringe to produce a dark red solution of (TPP)Zr(^{n}Bu)$_2$. ^{1}H-NMR (300 MHz, C_7D_8, see Fig. 3): δ −3.53 (t, J = 7.3 Hz, 4H, α-CH_2), −2.84 (quintet, J = 7.2 Hz, 4H, β-CH_2), −0.29 (sextet, J = 7.0 Hz, 4H, γ-CH_2), 0.15 (t, J = 7.2 Hz, 6H, δ-CH_3), 7.4–7.6 (m, 12H, *m*, *p*-phenyl), 7.88 (br d, 4H *o*-phenyl), 8.52 (br d, 4H *o*-phenyl), 8.92 (s, 8H, pyrrole) [22].

5.5. Reaction of (POR)M(OAc)$_2$ with ^{n}BuLi

(TPP)Hf(OAc)$_2$ (16.8 mg, 0.0185 mmol) was dissolved in C_7D_8 (1.0 ml) and a solution of ^{n}BuLi (2.5 M) was injected in two increments of 14.8 μl (2 equiv., 0.370 mmol) each via a 50 μl syringe. ^{1}H-NMR of the dark red solution resulting after the addition of the first increment is shown in Fig. 4(b), and the integrated ratio of metal coordinated ^{n}Bu to (TPP)Hf unit is 0.3:1. The ^{1}H-NMR spectrum of the dark red/brown solution obtained after the addition of the second increment is shown in Fig. 4(c), where the integrated ratio of coordinated ^{n}Bu to (TPP)Hf unit becomes 2:1, and is assigned to (TPP)Hf(^{n}Bu)$_2$. Similar observations were obtained on incremental addition of ^{n}BuLi to (TPP)Zr(OAc)$_2$, where the ratio of coordinated ^{n}Bu to (TPP)Zr unit was 0.1:1 after the addition of the first increment, and 2:1 after the addition of the second; and for (OEP)Zr(OAc)$_2$, where the ratio of coordinated ^{n}Bu to (OEP)Zr unit was 0.8:1 after addition of the first increment, and 2:1 after addition of the second. (TPP)Hf(^{n}Bu)$_2$: ^{1}H-NMR (500 MHz, C_7D_8, TPP and ^{n}Bu regions): δ −3.83 (t, J = 7.4 Hz, 4H, α-CH_2), −2.00 (quintet, J = 7.2 Hz, 4H,

β-CH_2), −0.19 (sextet, $J = 7.2$ Hz, 4H, γ-CH_2), 0.17 (t, $J = 7.2$ Hz, 6H, δ-CH_3), 7.3–7.6 (m, 12H, *m*, *p*-phenyl), 7.90 (br d, 4H *o*-phenyl), 8.47 (br d, 4H *o*-phenyl), 8.94 (s, 8H, pyrrole). (TPP)Zr(^{n}Bu)$_2$: ^{1}H-NMR (300 MHz, C_7D_8, TPP and ^{n}Bu regions): resonances identical to those obtained from the addition of 2 equiv. ^{n}BuLi to (TPP)$ZrCl_2$. (OEP)Zr(^{n}Bu)$_2$: ^{1}H-NMR (300 MHz, C_7D_8, OEP and ^{n}Bu regions): δ −3.87 (t, $J = 7.3$ Hz, 4H, α-CH_2), −3.01 (quintet, $J = 7.2$ Hz, 4H, β-CH_2), −0.45 (sextet, $J = 7.0$ Hz, 4H, γ-CH_2), 0.12 (t, $J = 7.2$ Hz, 6H, δ-CH_3), 1.88 (t, 24H, Et), 4.00 (m, 16H, Et), 10.53 (s, 4H, meta-porphyrin).

5.6. Reaction of (TPP)Zr(^{n}Bu)$_2$ with $PhMe_2SiH$

(TPP)$ZrCl_2$ (73 mg, 0.094 mmol) was allowed to react with ^{n}BuLi (0.10 ml, 2.0 M) in C_7D_8 to form (TPP)Zr(^{n}Bu)$_2$, the presence of which was verified by ^{1}H-NMR. Neat $PhMe_2SiH$ (5.0 μl, 3 equiv.) was added via a 10 μl syringe and the reaction mixture was warmed slowly in the NMR probe. The ^{1}H-NMR spectrum was recorded after every 20°C increment. Signals attributed to (TPP)Zr(^{n}Bu)$_2$ persisted up to 80°C, at which temperature decomposition occurred. No silicon containing products other than $PhMe_2SiH$ were observed.

5.7. Isolation of [(TPP)Zr(OH)$_2$]$_2$

A solution of (TPP)$ZrBu_2$ in C_6H_6, prepared from the reaction of (TPP)Zr(OAc)$_2$ with 4.0 equivalents of ^{n}BuLi, was stored for 1 month at 5°C. The resulting cubic shaped purple crystals were marginally soluble in $CDCl_3$. The structure was determined by single crystal X-ray diffraction to be a benzene solvate of [(TPP)Zr(μ-OH)$_2$]$_2$. ^{1}H-NMR (500 MHz, $CDCl_3$): δ 8.42 (s, 16H, pyrrole), 7.5–7.7 (m, 40H, Ph), −6.79 (s, μ-OH); IR(KBr): 3577 cm^{-1} (w, O–H).

5.8. Crystallographic data collection and structure determination

A crystal of dimensions 0.10 × 0.10 × 0.05 mm was mounted on a glass fiber in a random orientation. Preliminary examination and data collection were performed using a Siemens P4RA automated single crystal X-ray diffractometer using graphite monochromatic Mo Kα radiation ($\lambda = 0.71073$ Å) at 25°C. Autoindexing of 15 centered reflections from the rotation photographs indicated a triclinic lattice. Equivalent reflections were checked to confirm the Laue symmetry and a fractional index search was conducted to confirm the cell lengths XSCANS [23]. Final cell constants and orientation matrix for data collection were calculated by least squares refinement of the setting angles: 26 reflections ($12° < 2\theta < 26°$). Intensity data were collected using 2θ–θ scans with variable scan speed. Three representative reflections were measured every 50 reflections during data collection. Crystal data and intensity data collection parameters are listed in Table 1.

Data reduction was carried out using XSCANS and structure solution was achieved using the SHELXTL-PLUS (VMS) software package [24]. Empirical absorption correction was applied to the data. The structure was solved by Direct Methods and refined successfully in the space group $P\bar{1}$. Full matrix least-squares refinement on F^2 was carried out using SHELXL-93 [25]. The non-hydrogen atoms were refined anisotropically to convergence. The hydrogen atoms were calculated using riding models, but attempts to resolve disorder in the bridging oxygen atoms were not successful. The compound crystallizes with one molecule of benzene solvent per dimer, and the solvent molecule was disordered as well.

Projection views of the molecule with non-hydrogen atoms represented by 50% probability ellipsoids, and showing the atom labeling, are presented in Fig. 5. Experimental data, a complete list of bond distances, bond angles and positional and isotropic displacement coefficients for the non-hydrogen atoms are available from the authors and will be deposited with the Cambridge Structural Database. Additionally, two figures containing a labeled ORTEP diagram and a packing diagram are available from the authors.

Acknowledgments

Acknowledgment is made to the donors of the Petroleum Research Fund, administered by the American Chemical Society, and to the National Science Foundation (CHE-9213688) for partial support of this work. Financial support for JLH was provided by a UM-St. Louis Graduate School Summer Fellowship, and a Mallinkrodt Fellowship. Additional support was provided by a Research Incentive Award from the University of Missouri-St. Louis. We wish to thank C. Spilling and L. Brammer for helpful discussions and R. Guillard for a sample of H_2(OEP).

References and notes

[1] J.W. Buchler, in D. Dolphin (ed.), *The Porphyrins*, Vol. 1, Academic Press, New York, 1978, Chapter 10, p. 389.

[2] *cis* forms of (POR)MCl_2 for M = Zr, Hf: (a) (TPP)$ZrCl_2$(THF): H.-J. Kim, D. Whang, K. Kim and Y. Do, *Inorg. Chem.*, *32* (1993) 360. (b) (TPP)$HfCl_2$(0.5C_7H_8) and (OEP)$HfCl_2$(0.5CH_2Cl_2): S. Ryu, D. Whang, J. Kim, W. Yeo and K. Kim, *J. Chem. Soc. Dalton Trans.* (1993) 205. (c) (OEP)$ZrCl_2$(0.5C_7H_8): H. Brand and J. Arnold, *Organometallics*, *12* (1993) 3655.

[3] H. Brand and J. Arnold, *J. Am. Chem. Soc.*, *114* (1992) 2266.

[4] K. Shibata, T. Aida and S. Inoue, *Tetrahedron Lett., 33* (1992) 1077.
[5] J. Arnold, S.E. Johnson, C.B. Knobler and M.F. Hawthorne, *J. Am. Chem. Soc., 114* (1992) 3996.
[6] (a) S. Ryu, J. Kim, H. Yeo and K. Kim, *Inorg. Chim. Acta, 228* (1995) 233. (b) S. Ryu, D. Whang, H. Yeo and K. Kim, *Inorg. Chim. Acta, 221* (1994) 51.
[7] H. Brand, J.A. Capriotti and J. Arnold, *Organometallics, 13* (1994) 4469.
[8] (a) (OEP)$Zr(OAc)_2$: Full structural details have not been published, but a preliminary report appears in: M. Tsutsui and G.A. Taylor, in K.M. Smith (ed.), *Porphyrins and Metalloporphyrins*, Elsevier, Amsterdam, 1975, p. 295. (b) (TPP)$Zr(OAc)_2$: J.L. Huhmann, J.Y. Corey and N.P. Rath, *Acta Crystallogr., C51* (1995) 195.
[9] K. Shibata, T. Aida and S. Inoue, *Chem. Lett.* (1992) 1173.
[10] J.W. Buchler, in D. Dolphin (ed.), *The Porphyrins*, Vol. 1, Academic Press, New York, 1978, Chapter 10, p. 415.
[11] (a) (TPP)$ZrCl_2$ has been isolated from reaction of H_2(TPP) with $ZrCl_4$ in benzonitrile; B.D. Berezin and T.N. Lomova, Russ. *J. Inorg. Chem., 26* (1981) 203. (b) (TPP)$HfCl_2$ has been isolated from reaction of H_2(TPP) with $HfCl_4$ in phenol; T.N. Lomova, N.I. Volkova and B.D. Berezin, *Russ. J. Inorg. Chem., 28* (1983) 1429.
[12] J.W. Buchler, G. Eikelmann, L. Puppe, K. Rohbock, H.H. Shneehage and D. Weck, *Liebigs Ann. Chem., 745* (1971) 135.
[13] H.-J. Kim, D. Whang, Y. Do and K. Kim, *Chem. Lett.* (1993) 807.
[14] J.W. Buchler and K. Rohbock, *Inorg. Nucl. Chem. Lett., 8* (1972) 1073.
[15] T. Takahashi, M. Hasegawa, N. Suzuki, M. Subari, C.J. Rousset, P.E. Fanwick and E.I. Negishi, *J. Am. Chem. Soc., 113* (1991) 8564.
[16] (a) J.Y. Corey, J.L. Huhmann and X.H. Zhu, *Organometallics, 12* (1993) 1121. (b) J.Y. Corey and X.H. Zhu, *Organometallics, 11* (1992) 672. (c) J.Y. Corey, X H. Zhu, T.C. Bedard and L.D. Lange, *Organometallics, 10* (1991) 924.
[17] An ORTEP plot showing the disordered benzene solvent molecule is available from the authors.
[18] J. Arnold, C.G. Hoffman, D.Y. Dawson and F.J. Hollander, *Organometallics, 12* (1993) 3645.
[19] B. Cheng, J.D. Hobbs, P.G. Debrunner, J. Erlebacher, J.A. Shelnutt and W.R. Scheidt, *Inorg. Chem., 34* (1995) 102.
[20] J.D. Andose, A. Rauk, K. Mislow, *J. Am. Chem. Soc., 96* (1974) 6904.
[21] A.D. Adler, F.R. Longo, J.D. Finarelli, J. Goldmacher, J. Assour and L. Korsakoff, *J. Org. Chem., 32* (1967) 476.
[22] NMR data for (TPP)$Zr(^nBu)_2$ reported in Ref. [9]: ^{1}H-NMR (300 MHz, C_6D_6): δ −3.15 (t, 4H, α-CH_2), −2.51 (m, 4H, β-CH_2), 0.04 (m, 4H, γ-CH_2), 0.42 (t, 6H, δ-CH_3).
[23] XSCANS, Siemens Analytical Instruments, Madison, WI, (1994).
[24] SHELXTL- PLUS (VMS), G.M. Sheldrick, Madison, WI, 1991.
[25] SHELXTL, G.M. Sheldrick, Madison, WI, 1993.